RASĀYAN *J. Chem.*
Vol. 19 | No. 2 | 1060-1068| April-June | 2026
ISSN: 0974-1496 | e-ISSN: 0976-0083 | CODEN: RJCABP
http://www.rasayanjournal.com
http://www.rasayanjournal.co.in

SCHIFF BASE COMPLEXES WITH 2-CHLOROBENZALDEHYDE AND 1,3-DIAMINOPROPANOL: STRUCTURAL INSIGHTS, COMPUTATIONAL STUDIES AND MOLECULAR DOCKING AGAINST JN.1 RBD PROTEIN

S. R. Barik[1], P. K. Mohapatra[1,✉], and R. K. Mohapatra[2]
[1]Department of Chemistry, CV Raman Global University, Bhubaneswar-752054, (Odisha) India
[2]Department of Chemistry, Government College of Engineering,
Keonjhar-758002, (Odisha) India
✉Corresponding author: pkmohapatra@cgu-odisha.ac.in

ABSTRACT
Three metal-based compounds were prepared with a Schiff base (SB), obtained by interacting with 2-chlorobenzaldehyde and 1,3-diaminopropanol. The structure [$MLCl_2$] of the metal complexes was determined by using UV–vis, FT-IR, TGA, and ^1H & ^{13}C NMR studies. The metal-to-ligand ratio is found to be 1:1 molar ratio in the present compounds, as revealed by elemental analysis and spectroscopic data. Density functional theory (DFT) calculations were made to understand the bond length, bond parameters, bond angle and dihedral angles of these studied compounds. The MEP (molecular electrostatic potential) diagram for the compounds was studied to know the critical sites on the compounds for electrophilic attack. Moreover, the atomic charges were analysed to describe the physicochemical properties of these studied compounds. The docking study was performed against the PDB ID: 8YZD (JN.1 RBD protein in complex with ACE2). As per the findings, these four coordinated metal complexes showed greater binding affinity than the free ligand. The results of the study will help to develop potential inhibitors against SARS-CoV-2 variants, after further *in vitro* and *in vivo* validation.
Keywords: SB Ligand, Metal Complexes, Structural Insights, Computational Studies, Molecular Docking Study.
RASĀYAN *J. Chem.*, Vol. 19, No.2, 2026

INTRODUCTION

The SB compound was first reported by Hugo Schiff, who made it by condensing carbonyl compounds with aromatic/aliphatic primary amines.[1] These are stable imines which contain the C=N (azomethine) group. The presence of the 'N' atom (basic donor) in the azomethine group, the key component, can bind several metal ions with variable oxidation states.[2] Due to simplicity in metal complexation and synthesis, such ligands are gaining significant attention among the inorganic chemist community. Such types of ligands show exceptional ligating properties with metal ions due to the formation of a chelating environment around the central atom in the coordination sphere, and regulate the properties of the compounds.[3] The SB ligands form a large number of coordination compounds of various metals with structural diversity, having versatile applications in potential areas such as catalysis, biology, medicine, etc. Along with their broad industrial applications, such ligands and their metal complexes exhibit several physiological activities like antimicrobial, antiviral, anti-inflammatory, antipyretic, and antiproliferative properties.[4] Keeping in mind, we have synthesised and characterised one SB ligand and three metal [Ni(II), Cd(II), and Cu(II)] complexes in this study. Notably, SARS-CoV-2 variants are emerging continuously, and the ability of current drugs and vaccines is reduced in managing COVID-19. So, researchers are continuously working to find novel antiviral drugs to control the situation and any such possible situations in future. Due to this, we have performed a docking study for these synthesised compounds against the SARS-CoV-2 JN.1 RBD protein in complex with ACE2.

EXPERIMENTAL

The used chemicals, including 2-chlorobenzaldehyde, 1,3-diaminopropanol, metal salts, and various solvents, were of AR grade. The elemental (CHN) analysis was performed by using an Elementar Varrio

EL analyser. Infrared spectra were noted on a Perkin Elmer 621 spectrophotometer within a 4000–400 cm^{-1} range, with KBr to prepare the pellets. A thermal study was conducted by using thermogravimetric analysis on an SDTQ-600 system, at a 0–800 °C temperature range.

Procedure for the Synthesis of the Studied Compounds

The SB ligand (L) was synthesised from 2-chlorobenzaldehyde and 1,3-diaminopropanol, as reported by Azam and coworkers.[5] The solution of SB ligand (1 mml) in CH_2Cl_2 was dropwise added to metal chloride solution (M = Ni(II), Cd(II), Cu(II)) (1 mmol) with stirring for 30 minutes, maintaining a 1:1 molar ratio. It was concentrated under reduced pressure. To cause precipitation, n-hexane was added to the above solution. It was recrystallised to obtain the analytically pure form for further analysis (Scheme-1).

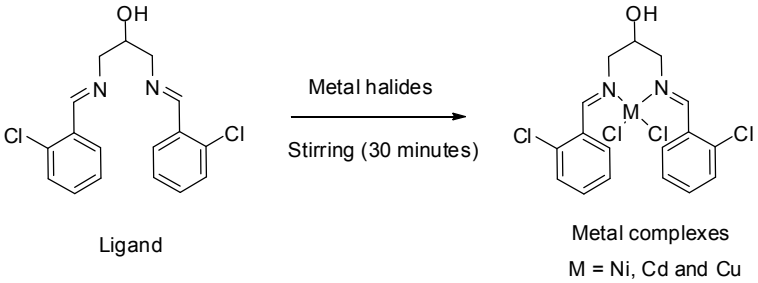

Scheme-1: Preparation of SB Metal Complexes

Complex-1: $[NiLCl_2]$: CHN data: (Calculated) C, 43.90; H, 3.44; N, 6.02; Found: C, 43.97; H, 3.47; N, 6.08

Complex-2: $[CdLCl_2]$: CHN data: (Calculated) C, 39.35; H, 3.08; N, 5.40; Found: C, 39.41; H, 3.12; N, 5.45

Complex-3: $[CuLCl_2]$: CHN data: (Calculated) C, 43.45; H, 3.40; N, 5.96; Found: C, 43.53; H, 3.46; N, 6.01

RESULTS AND DISCUSSION

IR Spectroscopy

Figure-1 shows the infrared spectrum of the nickel complex, highlighting its characteristic absorption bands. The band, due to the OH group appearing at nearly 3520 cm^{-1} (remains unchanged) in these studied metal-based compounds compared to the free SB, suggests that the OH group did not participate in complexation.[5] The band due to CH=N appearing nearly at 1550 cm^{-1} is shifted to low-frequency (in Ni(II), Cd(II), Cu(II) complexes) indicates its coordination to metal ion. These vibrations are essential to understand the electronic structure of the system and the interaction between the metal centre and the SB ligand.

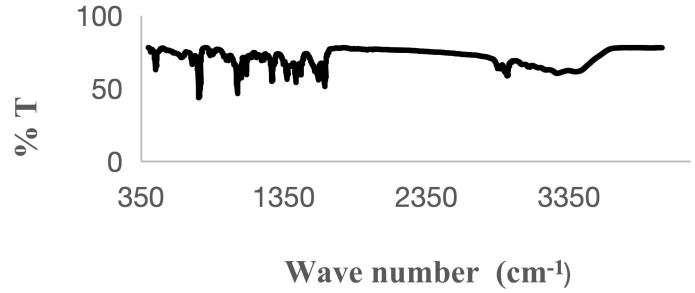

Fig.-1: A Representative FT-IR Spectrum of $[NiLCl_2]$ Complex

Thermogravimetric Analyses

TGA analysis (at heating rate of 10°C/min) of the cadmium complex was conducted in the range 0°C - 800°C (Fig.-2). The TGA curve revealed three distinct phases. In Phase 1, from 0°C to 220°C, there is almost no weight loss, indicating the complex remains stable up to 220°C, with no significant decomposition or evaporation. However, the minimal mass loss could be attributed to the evaporation of

adsorbed moisture or surface-bound water molecules. The lack of significant weight loss suggests that the material doesn't contain highly volatile components. However, a sharp decrease in mass is observed from 220-400°C, suggesting the thermal degradation of the organic components. From 400 to 550°C, the curve was slightly stable and after 550°C, the complex experiences a more gradual weight loss until 710°C, which is likely due to the breakdown of more heat-resistant organic residues or inorganic components. After this, there is a straight line indicating no further decomposition, which may be due to remaining thermally stable CdO.

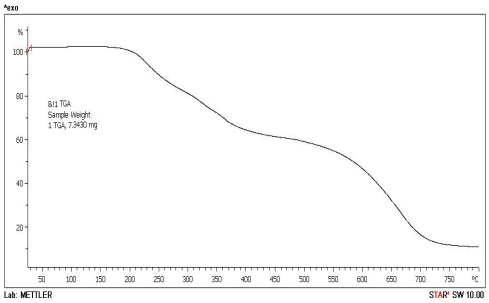

Fig.-2: TGA Spectra of [$CdLCl_2$] Complex

^{1}H and ^{13}C NMR Spectra

The SB ligand displayed a characteristic singlet at 8.55 ppm in the representative ^{1}H NMR spectrum, attributed to the –CH=N (azomethine) proton. Multiplet signals corresponding to the –CH_2 groups (4H) appear in the range of 3.09–4.21 ppm, while a singlet at 4.11 ppm is assigned for the –CH proton. A broad signal at 4.32 ppm is indicative of the –CH–OH group. Aromatic protons resonate at 6.89 - 7.27 ppm. In the ^{13}C NMR spectrum, the –CH_2, –CH–OH, and azomethine carbons are observed at 65.4 ppm, 70.58 ppm, and 160.1 ppm, respectively. Aromatic carbon signals are located in the range of 125.1–133.2 ppm. Upon complexation, the NMR spectra of the metal complex exhibit a notable downfield shift in both proton and carbon signals, confirming coordination of SB to the metal centre.

UV–vis Spectra

The obtained UV–vis spectra for these reported compounds were recorded at room temperature, using DMSO. The metal complexes showed four types of absorption peaks. The complexes showed broad d-d transitions at 575 nm ($^1A_{1g}\rightarrow{}^1A_{2g}$ transition) for the Ni(II) complex, and at 560 nm ($^2B_{1g}\rightarrow{}^2E_g$ transition) for the Cu(II) complex.[6] However, the charge transfer bands occurred (L→M) at 438 nm for the nickel complex, at 411 nm for the copper complex and at 450 nm for the Cd(II) complex.[7] Moreover, other bands for π -π* and n–π* transitions were also recorded for these metal-based compounds, indicating coordination between SB and metal ions in metal complexes. Based on these electronic spectral data, the studied metal complexes were assigned a square planar geometry.[8,9]

DFT Calculations

These compounds were subjected to full geometry optimisation using B3LYP in combination with 6-311++G(d,p) basis set for the non-metal atoms (H, C, N, O, and Cl), while LANL2DZ was used for the transition metal centres.[10-12] The electronic structures were explored from the frontier molecular orbitals (HOMO and LUMO). Based on these results, further quantum chemical descriptors were determined.[13] The optimised geometries of the SB ligand as well as its metal derivatives are presented in Fig.-3. The calculations indicate that the metal complexes adopt a four-coordinate arrangement around the metal ion with a general [$MLCl_2$] configuration, as illustrated in Fig.-3. The associated structural parameters are summarised in Table-1.

Frontier molecular orbitals (FMOs) represent the key electronic states that govern the chemical behaviour of a molecule. In particular, HOMO and LUMO are related to molecular reactivity. The spatial distribution of these orbitals for the SB and its metal complexes is illustrated through the three-dimensional visualisations provided in Fig.-4. Negative values of these orbitals are generally associated with enhanced molecular stability. The HOMO-LUMO energy difference (ΔE) is particularly significant as it governs electrical conductivity, optical polarizability, kinetic stability and reactivity parameters such as chemical hardness and softness (Fig.-4).

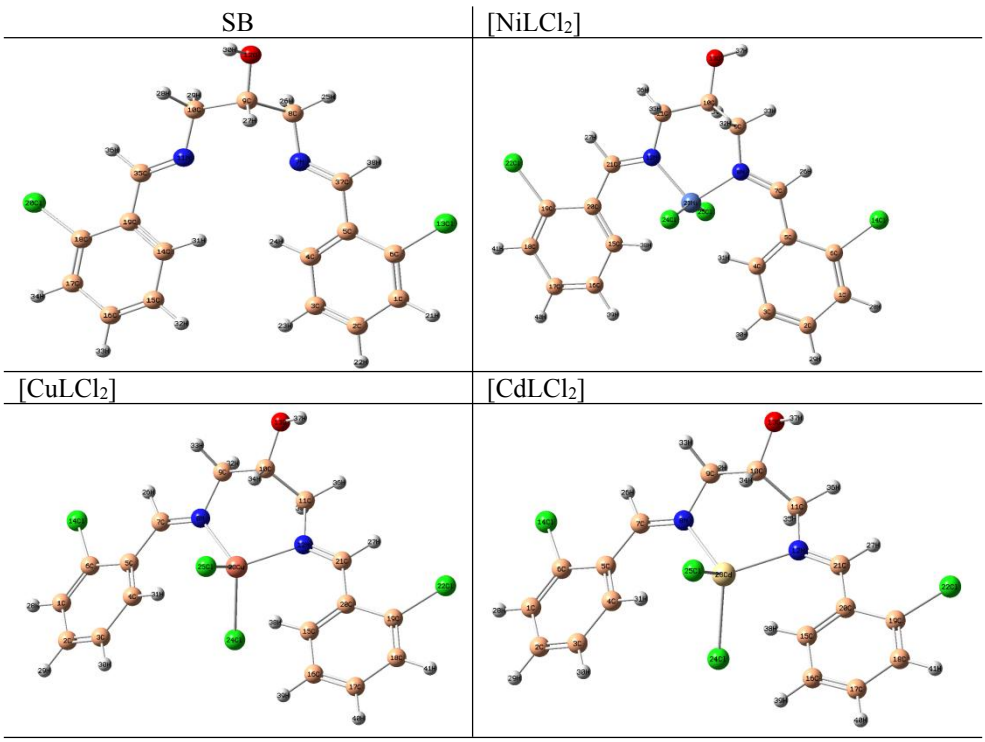

Fig.-3: 3D of SB and its Metal Complexes

Hardness and softness provide a measure of how a molecule accommodates charge redistribution, thereby reflecting its intrinsic reactivity.[14] Table-1 summarizes the calculated quantum descriptors for SB and its studied metal-based compounds, covering their electronic and structural parameters. The HOMO and LUMO energies are especially important, as a reduced energy gap (ΔE) is commonly linked to higher reactivity. In this regard, the Ni(II) complex exhibits the narrowest ΔE relative to the free ligand, indicating a pronounced increase in reactivity. The Cu(II) complex also displays a decrease in ΔE, though less dramatic, pointing to moderately enhanced reactivity. By contrast, the Cd(II) complex shows a slightly larger ΔE than the free ligand, suggesting a lower tendency for chemical reactivity.[15] Ionisation potential (I) and electron affinity (A) were also evaluated, since these properties describe the ability of a molecule to lose or accept electrons. A larger ionisation potential reflects weaker electron-donating ability, whereas a higher electron affinity indicates stronger electron-accepting capacity. The Ni(II) complex demonstrates a marked rise in ionisation potential, implying reduced electron donation, while the Cu(II) and Cd(II) complexes display more moderate variations. These differences in I and A highlight how metal coordination alters the electron transfer characteristics of the ligand.

The calculated chemical hardness (η) and softness (σ) provide further insights into stability and polarizability. Greater hardness is associated with higher stability, while increased softness reflects greater adaptability of the electron cloud. The Ni(II) complex exhibits a substantial rise in hardness, consistent with enhanced thermodynamic stability, whereas the Cu(II) and Cd(II) complexes show milder changes. Such variations are attributable to the redistribution of electronic density upon metal-ligand coordination. The electrophilicity index (ω) was also examined as a descriptor of a compound's tendency to act as an electrophile. Higher values denote stronger electrophilic character. Both Ni(II) and Cu(II) complexes exhibit increased ω, indicating a greater likelihood of engaging in electrophilic interactions compared to the free ligand, while Cd(II) shows only marginal variation. Overall, the analysis of these quantum chemical descriptors reveals that coordination to transition metals markedly influences electronic properties and reactivity of the SB ligand. Among the studied systems, the Ni(II) complex displays the most striking modifications in HOMO, LUMO, ΔE, ionisation potential, and hardness, suggesting a combination of enhanced stability and higher reactivity.

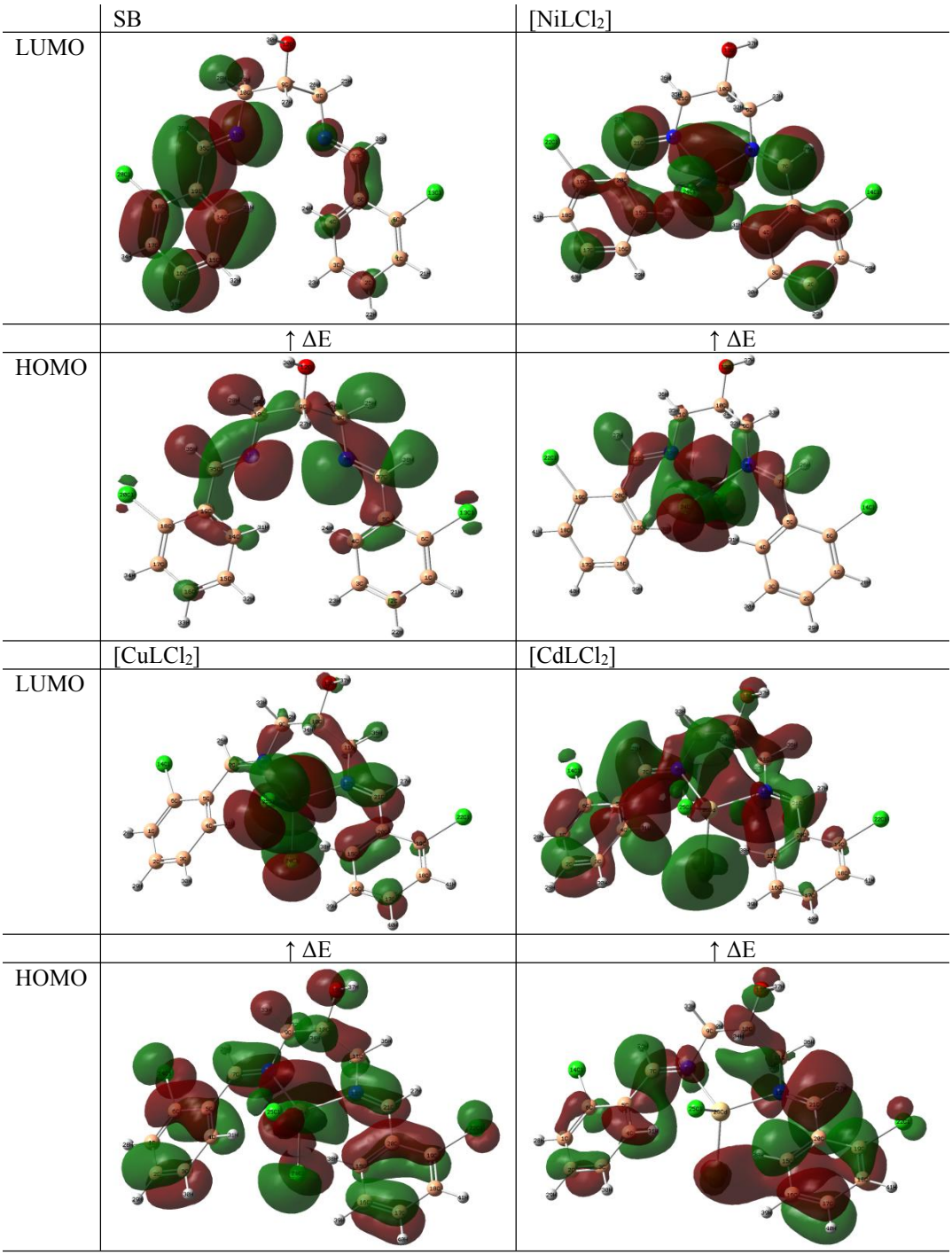

Fig.-4: HOMO-LUMO of SB and its Metal Complexes

Molecular Electrostatic Potential (MEP)

Both proteins and their bound substrates possess partial charges, which strongly influence the effectiveness of their mutual binding interactions. The MEP map is a valuable tool for exploring topological and structural features of three-dimensional molecules, as it highlights the regions where nuclei or electron density exert the greatest effect on molecular geometry. In the MEP diagram, a continuous colour gradient, ranging from blue to red, represents the potential distribution across the molecular surface.

Table-1: Quantum Chemical Descriptors of SB and its Metal-Based Compounds

	E_{HOMO}	E_{LUMO}	ΔE	I	A	χ	CP	η	σ	ω
SB	-6.39	-1.82	4.57	6.39	1.82	4.11	-4.11	2.28	0.22	3.69
$[NiLCl_2]$	-6.35	-4.63	1.72	6.35	4.63	5.49	-5.49	0.86	0.58	17.52
$[CuLCl_2]$	-7.36	-5.79	1.57	7.36	5.79	6.57	-6.57	0.79	0.64	27.46
$[CdLCl_2]$	-5.45	-4.37	1.08	5.45	4.37	4.91	-4.91	0.54	0.93	22.40

The blue region corresponds to electron-deficient sites, reflecting areas of positive potential that are prone to electrophilic interactions, whereas the red regions mark electron-rich domains, indicating favourable sites for nucleophilic attack.[16] The intensity of the red colouration directly correlates with the magnitude of negative charge; as electron density increases, these regions become more susceptible to interactions with incoming electrophiles during chemical reactions. The MEP surface of the investigated systems is presented in Fig.-5. The strongest negative potential regions shown by red are predominantly localised around nitrogen and oxygen atoms within the ligand framework. These heteroatoms, enriched in electron density, serve as preferential sites for electrophilic attack. However, the positive potential zones depicted by blue are mainly concentrated around hydrogen atoms.

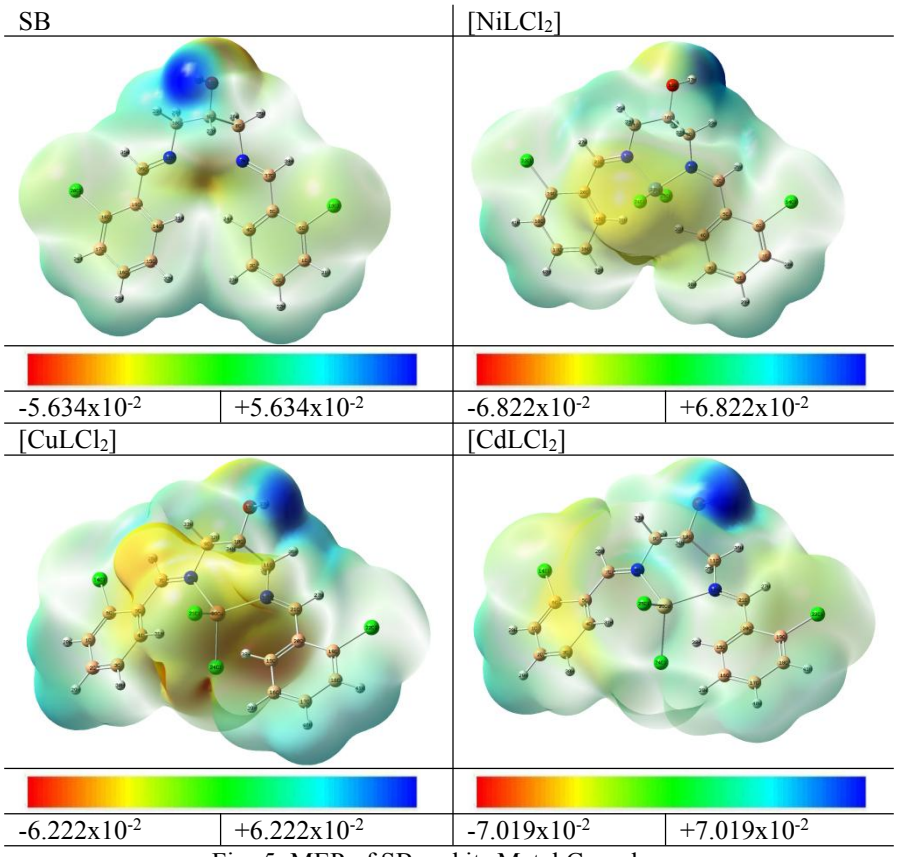

Fig.-5: MEP of SB and its Metal Complexes

Natural Charge Distribution (NBO)

Atomic charges are fundamental descriptors of molecules, as they directly influence their physicochemical behaviour, including electronic structure, vibrational characteristics, polarizability, dipole moment, and a wide range of related properties. In the present investigation, the atomic charges of SB and its metal complexes were determined through NBO analysis at B3LYP/6-311++G(d,p) level under gas-phase approximation. The outcomes are illustrated in Fig.-6. Among the studied systems, the

most pronounced negative charges are localised on heteroatoms such as oxygen, nitrogen, and chlorine, whereas the largest positive charges are associated with the hydrogen atoms.

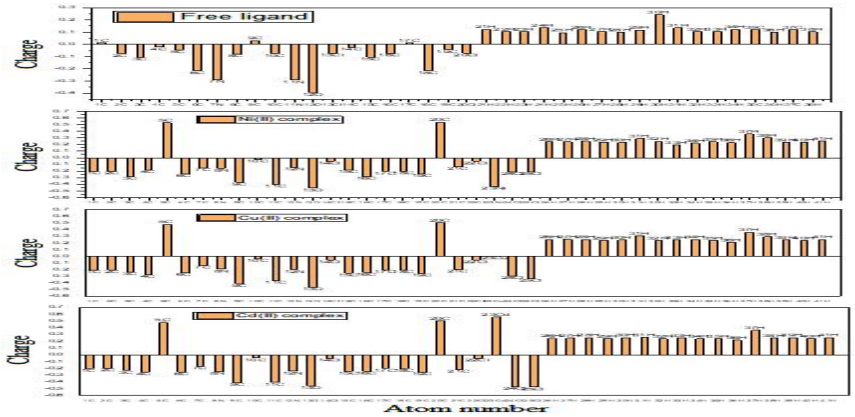

Fig.-6: The Plot of the Natural Charge Distribution of SB and its Metal Complexes in the Gas Phase

Molecular Docking Study

The protein-ligand docking study was reported by using AutoDock Vina (open source) software.[17,18] The 3D structure of JN.1 RBD protein in complex with ACE2 (protein) was obtained from https://www.rcsb.org/structure/8YZD. The ligands (studied compounds) were obtained in the .mol format (from DFT study) and converted to PDBQT format for the study. AutoDock tools were used to adjust Kollman charge, polar hydrogen and other parameters. The interactions of the studied compounds were visualised (with the best possible binding energy and the lowest docking score) by using Discovery Studio 3.5 (Fig.-7) and are given in Table-2. The predicted IC_{50} values (half-maximal inhibitory concentration) for the ligands were calculated with AutoDock v4.2 to know the ligand's specific potency in the inhibition (Table-2). All the studied ligands interacted with pdb id: 8YZD in the binding pocket cavity, with binding to the common amino acids PRO384 and LEU387. As per the results, the cadmium complex showed the best docking score of -8.99 kcal/mol and an IC_{50} value of 258.65 nM. So, further studies are recommended to validate the Cd(II) complex as the lead against the JN.1 RBD protein.

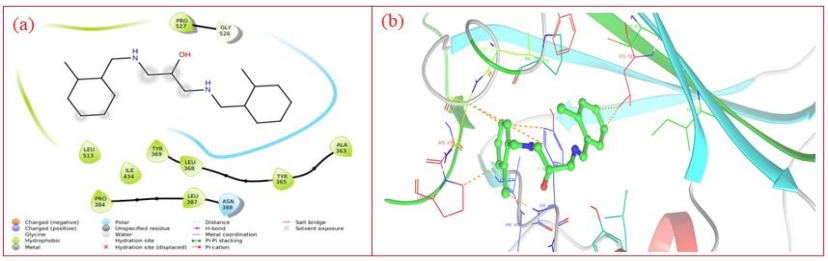

Fig.-7: 8YZD-SB Ligand Interactions: (a) 2D, (b) 3D

Table-2: Docking Results and the Interactions of the Compounds with 8YZD

Target	Compound	Binding Energy (kcal/mol)	Predicated IC50 Value	Interactions
PDB ID: 8YZD (Structure of JN.1 RBD	Ligand	-6.16	30.37 µM (micromolar)	ALA363, ASP364, TYR365, PRO384, LEU387, LEU513, GLY526, PRO527
	$[NiLCl_2]$	-8.64	465.07 nM (nanomolar)	ALA363, ASP364, TYR365, LEU368, PHE377, PRO384, THR385, LEU387, ASN388, ILE434, GLY526, PRO527

protein in complex with ACE2)	[$CuLCl_2$]	-8.12	1.12 µM (micromolar)	TYR365, SEP366, LEU368, TYR369, PRO373, PHE374, PHE375, PHE377, LYS378, PRO384, LEU387, ASN388, ILE434
	[$CdLCl_2$]	-8.99	258.65 nM (nanomolar)	TYR365, LEU368, TYR369, ALA372, PRO373, PHE375, PHE377, PRO384, LEU387, ASN388, ILE434, LEU513

CONCLUSION

Three SB metal complexes [$MLCl_2$] were successfully isolated. These compounds were characterised as per various spectroscopic studies. The DFT calculations for the compounds were done to study the electronic structure and stability of the coordination environment. The MEP diagram is also studied to know the most favourable part for an electrophilic attack. Moreover, the natural charge distribution of these compounds was computed to describe the physicochemical properties. As per the results of the molecular docking study, [$CdLCl_2$] showed the best docking score of -8.99 kcal/mol and IC_{50} value of 258.65 nM, which needs further validation.

ACKNOWLEDGMENTS

The authors acknowledged their respective institutions for the support.

CONFLICT OF INTERESTS

The authors declare that there is no conflict of interest.

AUTHOR CONTRIBUTIONS

The present work is related to *SDG-3: Good Health and Well-being*. All the authors contributed significantly to this manuscript, participated in reviewing/editing and approved the final draft for publication. The research profile of the authors can be verified from their ORCID IDs, given below:

Soumya R. Barik https://orcid.org/0000-0003-1562-1507
Pranab K. Mohapatra https://orcid.org/0000-0002-8898-8214
Ranjan K. Mohapatra https://orcid.org/0000-0001-7623-3343

Cite this article as: S. R. Barik *et al.*, *Rasayan J. Chem.*, 19(2), 1060-1068(2026), https://doi.org/10.31788/RJC.2026.1929574.

REFERENCES

1. C. Boulechfar, H. Ferkous, A. Delimi, A. Djedouani, A. Kahlouche, A. Boublia, A. S. Darwish, T. Lemaoui, R. Verma and Y. Benguerba, *Inorganic Chemistry Communications*, **150**, 110451(2023), https://doi.org/10.1016/j.inoche.2023.110451
2. R. K. Mohapatra, P. K. Das, M. K. Pradhan, M. M. El-Ajaily, D. Das, H. F. Salem, U. Mahanta, G. Badhei, P. K. Parhi, A. A. Maihub and K.-E. Zahan, *Comments on Inorganic Chemistry*, **39(3)**, 127(2019), https://doi.org/10.1080/02603594.2019.1594204
3. M. M. El-Ajaily, A. A. Maihub, U. K. Mahanta, G. Badhei, R. K. Mohapatra and P. K. Das, *Rasayan Journal of Chemistry*, **11(1)**, 166(2018), http://dx.doi.org/10.7324/RJC.2018.1111988
4. R. K. Mohapatra, P. K. Das, M. K. Pradhan, A. A. Maihub and M. M. El-ajaily, *Journal of the Iranian Chemical Society*, **15(10)**, 2193(2018), https://doi.org/10.1007/s13738-018-1411-2
5. M. Azam, I. Warad, S. Al-Resayes, M. Shakir, M. F. Ullah, A. Ahmad and F. H. Sarkar, *Inorganic Chemistry Communications*, **20**, 252(2012), https://doi.org/10.1016/j.inoche.2012.03.019

6. K. Jagadesh Babu, Dasari Ayodhya and Shivaraj, *Results in Chemistry*, **6**, 101110(2023), https://doi.org/10.1016/j.rechem.2023.101110
7. M. S. Begum, E. N. Zangrando, M. B. Howlader, M. C. Sheikh, R. Miyatake, M. M. Hossain, M. M. Alam and M. A. Hasnat, *Polyhedron*, **105**, 56(2016), https://doi.org/10.1016/j.poly.2015.11.046
8. G. A. El-Reash, O. A. El-Gammal, S. E. Ghazy and A. H. Radwan, *SpectrochimicaActa Part A: Molecular and Biomolecular Spectroscopy*, **104**, 26(2013), https://doi.org/10.1016/j.saa.2012.11.008
9. H. Ünver and Z. Hayvali, *Spectrochimica Acta Part A: Molecular and Biomolecular Spectroscopy*, **75(2)**, 782(2010), https://doi.org/10.1016/j.saa.2009.11.055
10. P. M. W. Gill, B. G. Johnson, J. A. Pople and M. J. Frisch, *Chemical Physics Letters*, **197(4-5)**, 499(1992), https://doi.org/10.1016/0009-2614(92)85807-M
11. M. W. Wong, P. M. W. Gill, R. H. Nobes and L. Radom, *The Journal of Physical Chemistry*, **92(17)**, 4875(1988), https://doi.org/10.1021/j100328a015
12. S. Chiodo, N. Russo, E. Sicilia, *The Journal of Chemical Physics*, **125**, 104107(2006), https://doi.org/10.1063/1.2345197
13. M. Hossain, K. Khushy, M. Latif, M.F. Hossen, M.A. Asraf, M. Kudrat-E-Zahan and A. Abdou, *Russian Journal of General Chemistry*, **92(12)**, 2723(2022), https://doi.org/10.1134/S1070363222120222
14. M. M. Khalaf, H. M. Abd El-Lateef, M. Gouda, A. A. Abdelhamid, M. Abdelbaset, A. H. Alsulami, M. N. Almarri, A. Abdou, *Computational Biology and Chemistry*, **109**, 108031(2024), https://doi.org/10.1016/j.compbiolchem.2024.108031
15. M. M. Khalaf, H. M. Abd El-Lateef, M. Gouda, A. A. Abdelhamid, A. A. Amer, A. Abdou, *ACS Omega*, **9(6)**, 6466(2024), https://doi.org/10.1021/acsomega.3c06274
16. M. Albqmi, N. A. Elkanzi, A. M. Ali, A. Abdou, *Journal of Molecular Structure*, **1319**, 139494(2025), https://doi.org/10.1016/j.molstruc.2024.139494
17. R. K. Mohapatra, A. Mahal, P. K. Mohapatra, A. K. Sarangi, S. Mishra, M. A. Alsuwat, N. N. Alshehri, S. M. Abdelkhalig, M. Garout, M. Aljeldah, A. A. Alshehri, A. Saif, M. A. Alshahrani, A. S. Alqahtani, Y. A. Almutawif, H. M. A. Eid, F. M. Albaqami, M. Abdalla, A. A. Rabaan, *Journal of Biosafety and Biosecurity*, **6(3)**, 157(2024), https://doi.org/10.1016/j.jobb.2024.05.004
18. N. M. El-Barasi, M. M. Miloud, M. M. El-ajaily, R. K. Mohapatra, A. K. Sarangi, D. Das, A. Mahal, P. K. Parhi, L. Pintilie, S. R. Barik, M. N. Bitu, *Journal of Saudi Chemical Society*, **24(6)**, 492(2020), https://doi.org/10.1016/j.jscs.2020.04.005

[RJC-9574/2026]